Neuron, Vol. 43, 539–549, August 19, 2004, Copyright ©2004 by Cell Press

Protein Kinase G Type II Is Required for Night-to-Day Progression of the Mammalian Circadian Clock

Shelley A. Tischkau,[1,2] Jennifer W. Mitchell,[2] Laura A. Pace, Jessica W. Barnes, Jeffrey A. Barnes, and Martha U. Gillette*
Department of Cell and Structural Biology
University of Illinois at Urbana-Champaign
B107 CLSL, 601 South Goodwin Avenue
Urbana, Illinois 61801

Summary

Circadian clocks comprise a cyclic series of dynamic cellular states, characterized by the changing availability of substrates that alter clock time when activated. To determine whether circadian clocks, like the cell cycle, exhibit regulation by key phosphorylation events, we examined endogenous kinase regulation of timekeeping in the mammalian suprachiasmatic nucleus (SCN). Short-term inhibition of PKG-II but not PKG-Iβ using antisense oligodeoxynucleotides delayed rhythms of electrical activity and *Bmal1* mRNA. Phase resetting was rapid and dynamic; inhibition of PKG-II forced repetition of the last 3.5 hr of the cycle. Chronic inhibition of PKG-II disrupted electrical activity rhythms and tonically increased *Bmal1* mRNA. PKG-II-like immunoreactivity was detected after coimmunoprecipitation with CLOCK, and CLOCK was phosphorylated in the presence of active PKG-II. PKG-II activation may define a critical control point for temporal progression into the daytime domain by acting on the positive arm of the transcriptional/translational feedback loop.

Introduction

The periodic recurrence of night and day provides a stable environmental context for life on earth. As life evolved within this environment, daily biological cyclicity was incorporated into the genome. Thus, circadian rhythms, or near 24 hr patterns of behavior and physiology driven by gene expression, are nearly ubiquitous among eukaryotic organisms. Endogenous circadian rhythmicity is characterized by its persistence under constant environmental conditions and its responsiveness to specific cues that enable synchronization to the solar cycle. In mammals, the primary circadian clock is located within the suprachiasmatic nucleus (SCN) of the basal hypothalamus. Although organismic rhythmicity is an emergent property of the SCN, individual cells contain clocks (Michel et al., 1993; Welsh et al., 1995). Circadian timekeeping emerges from a dynamic sequence of cellular events, organized into specific time domains, which are defined by divergent sensitivities to resetting stimuli. Underlying these domains are differences in activatable signal transduction pathways and dominant molecular and biochemical elements (Gillette, 1996; Gillette et al., 1995; Merrow et al., 1997). The molecular framework for these time domains is constructed from the coordinated function of a core group of clock genes, expressed as interlocking transcriptional/translational feedback loops containing both positive (*Bmal1* and *Clock*) and negative arms (*Per*/*Cry*/*Tim*) (Okamura et al., 2002).

The cell cycle is another molecular timing device found within biological systems. Similar to the circadian clock, the free-running period of mitosis is ~24 hr in many eukaryotic cells (Tyson et al., 2002). Cell replication is controlled by complex intracellular signaling pathways that integrate information about the extracellular environment with intracellular cues. The events of the cell cycle are predominantly controlled at the protein level by a small number of heterodimeric protein kinases. These kinases, which fluctuate over the course of the cycle, exert control over multiple proteins that are involved in transcription, DNA replication, and cytokinesis by phosphorylation at specific regulatory sites, rendering certain proteins active while inactivating others (Nurse, 2002; Tyson et al., 2002).

Knowledge of cell cycle regulation prompted our investigation of critical kinases for regulating the circadian clock. Clock elements are regulated by complex cellular processes that include posttranslational modifications of proteins by phosphorylation (Eide et al., 2002; Garceau et al., 1997; Kloss et al., 1998; Lee et al., 2001; Lin et al., 2001; Merrow et al., 1997; Okamura et al., 2002; Ripperger and Schibler, 2001). Phosphorylation of clock elements, accomplished by specific protein kinases, is clock state dependent (Garceau et al., 1997; Kloss et al., 1998, 2001; Lee et al., 2001; Lowrey et al., 2000; Martinek et al., 2001; Price et al., 1995; Yang et al., 2001) and characteristic of key events during clock resetting (Naidoo et al., 1999; Yang et al., 2001). Furthermore, experimental manipulation of kinase activity demonstrates the importance of specific kinases in the regulation of the circadian timing process (Comolli and Hastings, 1999; Eskin et al., 1984; Gillette and Mitchell, 2002; Krucher et al., 1997; Obrietan et al., 1998; Tischkau et al., 2000). Recently, we demonstrated clock-controlled regulation of cGMP-dependent protein kinase (protein kinase G, PKG) activity in the SCN (Tischkau et al., 2003b). Clock sensitivity to manipulation of cGMP-dependent signaling pathways is a conserved feature of the nocturnal domain (Eskin et al., 1984; Prosser et al., 1989). Activation of PKG is required during phase resetting induced by light (Mathur et al., 1996; Weber et al., 1995) and glutamate (Ding et al., 1998) in the late subjective night. Inhibition of the endogenous rise in PKG activity at the end of subjective night causes significant phase delays in the circadian rhythms of wheel running activity, SCN neuronal activity, cGMP levels, and *Per1* mRNA (Tischkau et al., 2003b).

We hypothesized that PKG activation defines a checkpoint, which is permissive for progression of the circa-

*Correspondence: mgillett@uiuc.edu
[1]Present address: Department of Veterinary Biosciences, University of Illinois at Urbana-Champaign, 3840 VMBSB, 2001 South Lincoln Avenue, Urbana, Illinois 61802.
[2]These authors contributed equally to this work.

dian clock at the end of the nocturnal domain. This role would be similar to G2/M cyclin-dependent kinase (CDK) control of progression from S phase in the cell cycle (Hayles et al., 1994). Our results provide compelling evidence for such a checkpoint at the night-to-day transition and suggest that passage through this checkpoint is dependent upon clock-controlled activation of PKG-II. If PKG-II activation fails to occur during this restricted interval, the clock rapidly resets to an earlier state and must repeat the late-night domain. Extended PKG inhibition increases in the magnitude of the delay by quantal increments, and constant inhibition of PKG-II disrupts SCN circadian rhythmicity. Finally, mechanistic studies indicate that PKG may act on the positive arm of the core molecular clockworks. Thus, increased activity of PKG-II specifically at the end of subjective night is required for night-to-day progression of the SCN circadian cycle.

Results

PKG-II in the SCN

PKG activity in the SCN exhibits an endogenous oscillation that peaks at the end of subjective night (Tischkau et al., 2003b). To determine which PKG isoform(s) is involved in clock regulation, we developed subtype-specific antibodies against sequences unique to PKG-Iα, -Iβ, or -II. The PKG-Iβ antibody detected a 78 kDa band corresponding to the mass of PKG-Iβ (78 kDa) (Pohler et al., 1995) only in the lanes containing recombinant PKG-Iβ (Alexis Biochemicals, San Diego, CA) (Figure 1A). The PKG-II antibody detects a band at ~80 kDa in human embryonic kidney 293 (HEK) cell extracts corresponding to endogenous PKG-II (Figure 1B). The expression of PKG-II is expected from a cell line derived from kidney, which is known to contain high levels of PKG-II (Gambaryan et al., 1996; Vaandrager et al., 1997), and we have determined that the HEK cell line expresses significant levels of PKG-II transcript (L.A.P. and M.U.G., unpublished data). Additionally, the PKG-II antibody detects a band at the predicted 86 kDa only in the lane loaded with PKG-II overexpressed in HEK cells. The difference in migration of this PKG-II protein is due to the addition of a hexahistidine (Vaandrager et al., 1997) (Figure 1B). Furthermore, Western blot analysis demonstrated that both PKG-Iβ and PKG-II are present in the rat SCN (Figures 1A and 1B). In SCN extracts, an additional lower band corresponding to a mass of ~70 kDa was detected in the PKG-II immunoblot. This band is also present in other rodent tissues and cell lines (unpublished data), but it is not crossreactive with antibodies against PKG-Iα or PKG-Iβ. The lower band is an undetermined by-product recognized by the PKG-II-specific antibody that can easily be identified by size. Finally, our anti-PKG-Iα antibody detected a band corresponding to the mass of PKG Iα (76 kDa) (Butt et al., 1993) in a lane loaded with PKG-Iα recombinant protein. However, no band was detected in lanes loaded with PKG-Iβ or PKG-II protein overexpressed in the HEK cell line or untransfected HEK cells. PKG-Iα was not detectable in SCN tissue by Western blot (data not shown).

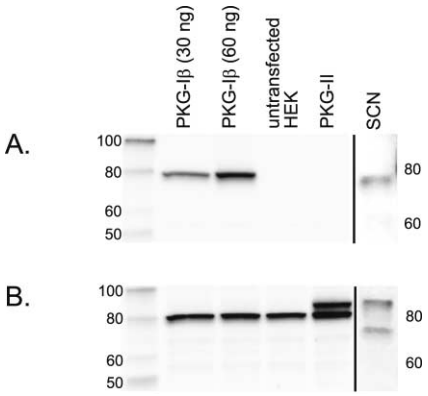

Figure 1. Isoform-Specific Antibodies Raised Against PKG-Iβ and PKG-II Detect PKG-1β and PKG-II in SCN Tissue

Immunoblots were loaded with 25 μg of total protein as follows (left to right): lane 1, molecular weight standards; lane 2, HEK293 cell extract plus 30 ng recombinant PKG-1β; lane 3, HEK293 cell extract plus 60 ng recombinant PKG-1β; lane 4, untransfected HEK293 extract; lane 5, HEK293 cells transfected with CMVneo-PKG-II; lane 6, SCN tissue extract. (A) PKG-Iβ antiserum detects a 78 kDa band in lanes loaded with HEK cell extracts plus either 30 or 60 ng of recombinant PKG-1β protein, as well as SCN extracts, but not samples of untransfected HEK cells or HEK transfected with CMVneo-PKG-II. (B) PKG-II antiserum detects an 86 kDa band in HEK cells that overexpress PKG-II, but not in HEK cells untransfected or containing the recombinant PKG-Iβ isoform. The SCN displays a band at ~86 kDa that corresponds to rat PKG-II protein. The additional band at ~70 kDa is an unidentified protein that was detected in SCN extracts. HEK cells also express an 80 kDa band that is the molecular weight of human PKG-II, which is expressed in kidney. Labels for each blot are as follows: untransfected HEK, HEK 293 cell lysate; PKG-1β, bovine recombinant PKG-Iβ in HEK cells; PKG-II, PKG-II overexpressed in HEK cells; SCN, SCN tissue extract.

Knockdown of PKG-II Resets the SCN Clock

Pharmacological inhibition of the spontaneous rise in PKG activity at the end of subjective night alters circadian timekeeping (Tischkau et al., 2003b). To determine which isoform of PKG mediates this effect, we used isoform-specific antisense oligodeoxynucleotides (αODN) (Barnes et al., 2003; Tischkau et al., 2003a) directed against the 5′ start site of the PKG-I or PKG-II mRNA. We examined the effects of αODN applied from circadian time (CT) 18 to CT 23 on the electrical activity rhythm in SCN brain slices. In control recordings, the ensemble of SCN neurons displayed a spontaneous rhythm in firing rate with a peak near CT 7 (time of peak = CT 6.72 ± 0.10, n = 8) for up to 3 days when maintained in vitro (Figure 2A). The time of peak is an established phase marker of the SCN circadian rhythm of electrical activity (Ding et al., 1994). Application of αODN against PKG-II caused a significant phase delay of this rhythm (Figures 2B and 2G, mean time of peak = CT 10.13 ± 0.19 hr, n = 4, $p < 0.01$). No effect on the SCN neuronal activity rhythm was observed after treatment with scrambled ODN (Figures 2C and 2G, CT 6.50 ± 0.14, n = 3) or PKG-II αODNs bearing three (Figures 2E and 2G, CT 6.58 ± 0.08, n = 3) or one (Figures 2D and 2G, CT 6.67 ± 0.22, n = 3) mismatched nucleotides. Furthermore, application of PKG-I αODN had no effect on SCN electrical activity rhythms (Figure 2F, CT 6.42 ± 0.17, n = 3), although 6 hr treatment with PKG-I αODN knocks PKG-1β protein levels down by 35% and func-

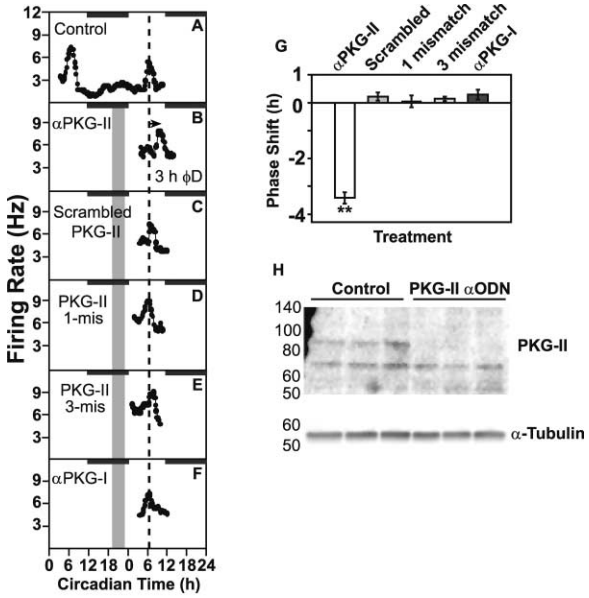

Figure 2. Knockdown of PKG-II by αODN Treatment from CT 19-23 Causes a Significant Delay in the SCN Rhythm

(A) A representative single-unit recording from the ensemble of SCN neurons shows an endogenous circadian rhythm in electrical activity that peaks at ~CT 7 on both day one and day two in vitro. The mean time of peak for control experiments, CT 6.72 ± 0.10 (n = 8), is the phase marker to which peak activity in experimentals was compared. The horizontal black bar indicates nighttime in the donor colony; 500 μm coronal hypothalamic slices were maintained in constant light. Vertical gray bars indicate the circadian time (CT) and duration of treatment.

(B) Isoform-specific αODN against PKG-II (αPKG-II, 10 μM) bath applied from CT 19–23 caused a significant delay in the time of peak for the SCN electrical activity rhythm on the subsequent day. Data shown are from a representative experiment. The average time of peak was CT 10.13 ± 0.19 (n = 4), which is significantly different from the time of peak in control recordings ($p < 0.01$, Student's t test). This represents a mean phase delay of −3.4 hr (panel [G]).

(C) Scrambled PKG-II ODN (10 μM) had no effect on the phase of the rhythm on the subsequent day. The average time of peak was CT 6.50 ± 0.14 (n = 3), which was not significantly different from the control time of peak (Student's t test).

(D) PKG-II αODN bearing one mismatched nucleotide (10 μM) had no effect on the phase (Student's t test). Mean time of peak was CT 6.67 ± 0.22 (n = 3).

(E) PKG-II αODN bearing three mismatched nucleotides (10 μM) had no effect (Student's t test). Mean time of peak was CT 6.58 ± 0.08 (n = 3).

(F) PKG-I αODN (10 μM) had no effect on SCN rhythmicity (Student's t test). Mean time of peak was CT 6.42 ± 0.17 (n = 3).

(G) Bar graph showing mean ± SEM for these experiments (n = 3–4). ** indicates statistical significance ($p < 0.01$) as determined by Student's t test.

(H) Western blot of individual SCN slices (n = 3 control, 3 treated with αODN against PKG-II) indicates a significant reduction in PKG-II levels after PKG-II αODN (10 μm) treatment from CT 1–23. Intensity of an uncharacterized lower band (70 kDa) is not affected by PKG-II αODN treatment. PKG-I αODN also significantly reduced PKG-Iβ protein levels (data not shown). Loading levels were evaluated by reprobing the blot with anti-α-tubulin antibody.

tionally inactivates it (data not shown). Chronic PKG-II αODN treatment effectively reduced the PKG-II levels in the SCN by 65% (Figure 2H). The PKG-II αODN treatment did not affect expression of the lower band (70 kDa) detectable by PKG-II immunobloting, further supporting our contention that the lower band is not PKG-II, but an unidentified protein that interacts with our primary antibody.

Dynamic Phase Resetting by PKG Inhibition

In our system, measurable phase delays could result from either (1) the clock stalling at the time of treatment and remaining at that point until the treatment is removed or (2) immediate clock resetting to an earlier time. To distinguish between these possibilities, we evaluated the effect of various durations of PKG inhibition and effects of double pulses of inhibitors. First, the PKG inhibitor KT5823 (1.0 μM) was applied for different durations at CT 22, the time of maximal sensitivity to phase shifting (Tischkau et al., 2003b). KT5823 was used for these experiments rather than PKG-II αODN because the duration of antisense treatment required for an effect is much longer than that for KT5823 (2 hr versus 15 min). Application of KT5823 for 0.25, 1, 2, or 3 hr beginning at CT 22 induced ~3.5 hr phase delay in the electrical activity rhythm that was stable over two circadian cycles (Figure 3A). However, exposure to KT5823 for 3.5 (n = 3) or 6 hr (n = 3), delayed the electrical activity rhythm by nearly 7 hr (−6.56 ± 0.45, −6.78 ± 0.33, respectively, Figures 3A and 3B). Therefore, the magnitude of the phase delay was not proportional to the duration of KT5823 exposure. Rather, the delay occurred in what appeared to be a step function: treatments <3.5 hr induced an ~3.5 hr phase delay, while treatments ≥3.5 hr induced a quantal increase in the delay, from 3.5 hr to 7 hr.

In a second set of experiments, KT5823 was applied in two discrete pulses (15 min each): one at CT 22 and a second either 1 hr later at CT 23 or 3.5 hr later at CT 1.5 (Figures 3A and 3B). A phase delay of −3.61 ± 0.33 (n = 3) was observed when the two pulses were separated by 1 hr. In contrast, separation of the two pulses by 3.5 hr caused a phase shift of −6.89 ± 0.25 hr (n = 3). Notably, these phase shifts were stable, as indicated by their persistence on the third day in vitro. These data are consistent with the hypothesis that phase resetting is dynamic; inhibition of PKG most likely resets the clock immediately to an earlier time, from which the clock resumes forward progression so that it again becomes sensitive to the PKG inhibition 3.5 hr later.

To further test the hypothesis that clock resetting is dynamic, we performed additional double-pulse experiments. A KT5823 pulse at CT 22 was followed by a pulse of glutamate, which causes phase advance when applied in the latter half of subjective night (Ding et al., 1994; Tischkau et al., 2000). As indicated in Figure 4A, if phase resetting is dynamic, we predicted that a pulse of glutamate applied 30 min after the pulse of KT5823 at CT 22 would cause a phase shift that corresponds to the summation of individual phase shifts initiated first by KT5823 at CT 22 (−3.5 hr) and then by glutamate at CT 19 (+3.5 hr); the result measured during the subsequent circadian cycle should be no shift in clock phase. No shift was observed when glutamate was applied 30 min following KT5823 at CT 22 (Figures 4B and 4C lane 5, green bar, time of peak = CT 6.84 ± 0.25, n = 4). Another prediction of this dynamic model is that a pulse of glutamate applied 3.5 hr following a pulse of KT5823 at CT

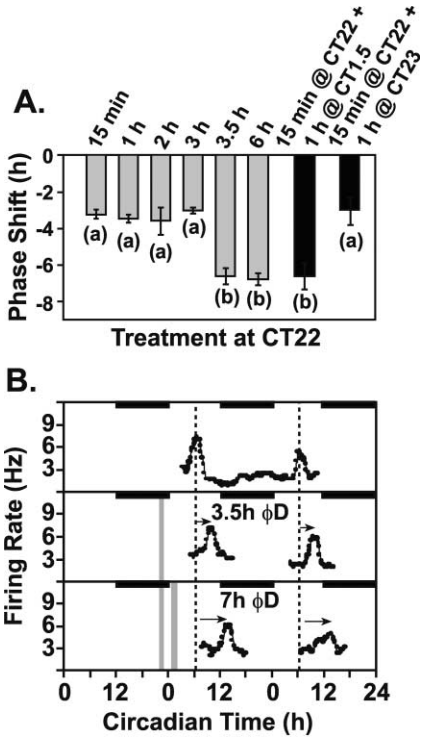

Figure 3. PKG Inhibition at the End of Subjective Night Causes Quantal Changes in the Magnitude of the Phase Shift of Electrical Activity Rhythms in SCN Brain Slices

(A) Responses to KT5823 treatments of various durations initiated at CT 22. Treatments of 0.25–3.0 hr caused ~3.5 hr phase delays in SCN electrical activity rhythms. Longer treatments, 3.5 and 6.0 hr in duration, caused ~7 hr phase delays in SCN electrical activity rhythms. Similarly, two treatments spanning the 3.5 hr treatment time caused an ~7 hr phase delay. Data are mean ± SEM time of peak neuronal activity, the phase marker, of three to six independent single-unit recording experiments. Bars with different letters (a or b) indicate treatments that are statistically different from each other ($p < 0.01$), as determined by ANOVA with Student-Neuman-Keuls post hoc analysis.

(B) Phase delays stimulated by KT5823 pulses are stable. Single-unit recordings in a representative control experiment show that the time of peak firing rate is the same on days 2 and 3 in vitro (top panel). When KT5823 was applied for either 1 hr at CT 22 of day 1 (middle panel) or for 15 min at CT 22 followed by a 1 hr treatment at CT 1.5 of day 2 (3.5 hr later) (lower panel), the respective 3.5 and 7 hr phase delays were stable over days 2 and 3. This indicates permanent resetting of the SCN circadian clock. Dashed line, time of peak in control SCN; arrow, magnitude of phase shift; ϕD, phase delay.

22 should result in a phase shift measured the following day that corresponds to the sum of effects of KT5823 at CT 22 (−3.5 hr) plus a glutamate-induced shift at CT 22 (+1.5 hr); the consequent shift should be −2 hr (Figure 4A). Indeed, such a phase delay (−1.72 ± 0.45 hr, n = 4) was observed when glutamate was applied 3.5 hr following KT5823 at CT 22 (Figures 4B and 4C, lane 6, green bar). These data strongly support the hypothesis that phase resetting caused by inhibiting PKG at CT 22 involves a dynamic, rapid alteration in clock state so that phase-appropriate sensitivity to glutamate reemerges.

PKG-II Is Required for SCN Circadian Rhythms

The previous experiment demonstrates that PKG-II is required for progression of the circadian clock at CT 22. To determine whether this emergence of PKG activity is required for circadian rhythmicity, αODN to either PKG-I or -II was applied continuously to the bath of the slice chamber while recording SCN single-unit activity. Under these conditions, PKG-II αODN suppressed the endogenous rhythm of spontaneous electrical activity of SCN neurons (Figure 5B, n = 5). A normal rhythm was observed in the presence of ODN containing an identical complement of nucleotides in a scrambled sequence (CT 6.53 ± 0.25, n = 4, Figure 5C) or an αODN against PKG-I (CT 6.74 ± 0.33, n = 4, Figure 5D). We conclude that suppression of the circadian rhythm was specific to PKG-II αODN treatment and the concomitant reduction of PKG-II expression.

To evaluate whether the αODN-induced inhibition of circadian rhythmicity is reversible, αODN to PKG-I or -II was applied to SCN slices for 22 hr from CT 2 to CT 24/0. Single-unit activity on the following day, after removal of the treatment, revealed the reemergence of the spontaneous electrical activity rhythm with a peak at CT 10.19 ± 0.16, (n = 4), a phase delay of −3.47 hr (Figure 5E). These data indicate that PKG-II only, and not PKG-Iβ, is required for the electrical activity rhythm of SCN neurons and that the sensitive period at the end of subjective night is the only domain that is sensitive to PKG-II inhibition. However, when PKG-II activation is blocked during this sensitive period, either during long-term exposure to PKG-II αODN or by a 15 min pulse of KT5823, the delay is 3.5 hr.

Effects of PKG-II on Positive Clock Elements, *Clock*, and *Bmal1*

Coimmunoprecipitation experiments were performed to assess the potential interaction of PKG-II with the core clock element, CLOCK, in vivo at the end of the night. Western analysis of SCN extracts obtained ex vivo at ZT 22 and subjected to coimmunoprecipitation with an antibody against CLOCK indicates PKG-II immunoreactivity (Figure 6A). PKG-II was not immunoprecipitated with nonspecific IgG. Furthermore, CLOCK is phosphorylated significantly in NIH 3T3 cells transfected with both wild-type PKG-II and CLOCK. Increased phosphorylation of CLOCK was observed in NIH 3T3 cells cotransfected with CLOCK and a constitutively active form of PKG-II (Figures 6B and 6C). Although these data were obtained from NIH 3T3 cells and not directly from the SCN, they provide evidence that CLOCK can act as a substrate for activated-PKG-II.

Because these data suggest an influence of PKG-II on the positive arm of the transcriptional/translational negative feedback loop at the end of the night domain, we evaluated the other element in the positive arm, *Bmal1*, after PKG αODN treatment. *Bmal1* mRNA levels in 500 μm SCN punches were measured by qPCR and normalized against a housekeeping transcript for acid ribosomal protein, NM022402. Endogenous expression of *Bmal1* exhibits clear circadian rhythmicity with a peak in the latter half of night under free-running conditions in the SCN in vitro (Figure 7). The *Bmal1* profile shows a sharp decline in transcript abundance toward the end of night. SCN slices treated with the PKG-II αODN from CT 2 to CT 24/0 exhibited changes consistent with resetting (3.5 hr) of the *Bmal1* rhythm. After removal of PKG-II αODN, *Bmal1* levels in SCN were low at predicted CT

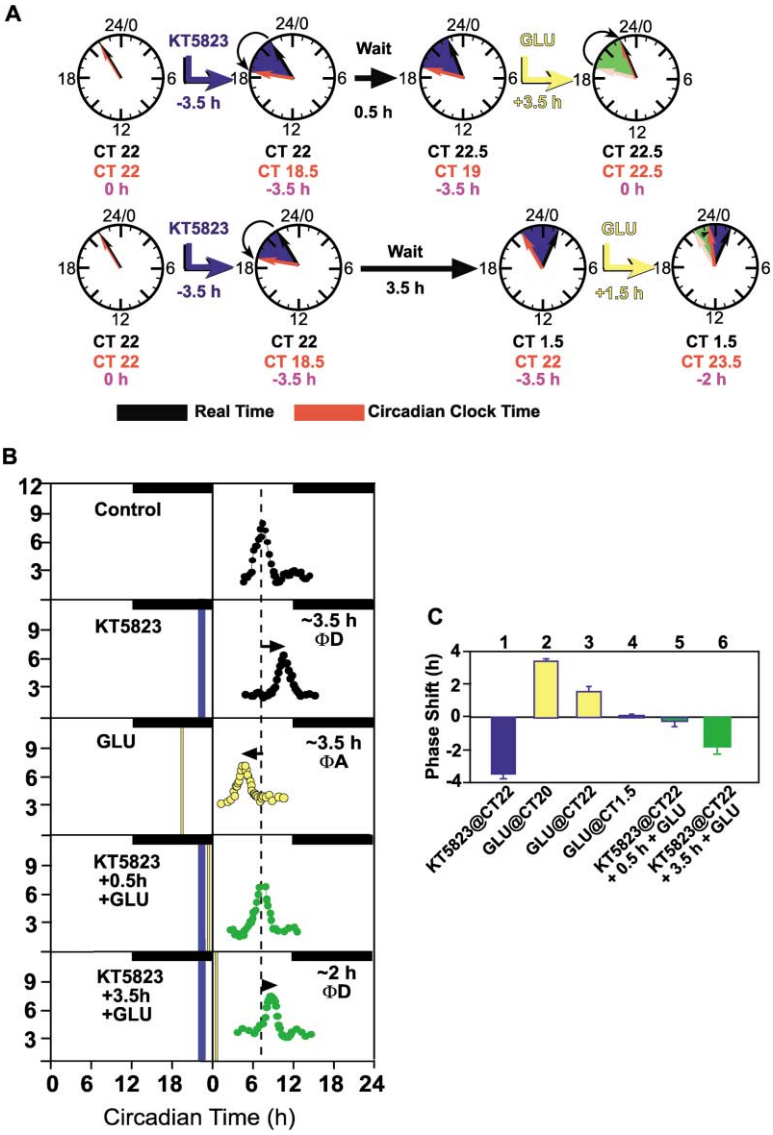

Figure 4. Double-Pulse Experiments with KT5823 and Glutamate Indicate Rapid, Dynamic Phase Resetting of the SCN Clock

(A) Theoretical model depicting the phase shifts predicted by the hypothesis that inhibition of PKG at CT 22 rapidly resets the clock back by 3.5 hr into an earlier time domain sensitive to phase resetting by glutamate (GLU).

(B) Representative recordings from SCN slices treated as indicated in the individual panels. Blue bars indicate time of KT5823 treatment. Yellow bars indicate time of GLU treatment. Treatment with KT5823 alone at CT 22 caused an ~3.5 hr phase delay. GLU treatments at CT 20 caused an ~3.5 hr phase advance. KT5823 followed by GLU within 30 min resulted in no change in phase on the subsequent day. KT5823 followed by GLU after a 3.5 hr interval caused an ~2 hr phase delay.

(C) Summary of actual phase shifts in SCN electrical activity rhythms observed after treatments based on the predictions made in (A) (n = 3 to 6 for each bar). Application of KT5823 at CT 22 induces a 3.5 hr phase delay, which predicts a rapid, dynamic phase shift that "sets" the clock back to CT 18.5. Actual recording data indicate that KT5823 applied at CT 22 causes a 3.5 hr phase delay ([C1], blue bar). Application of GLU (10 mM) at CT 19 induces a 3.5 hr phase advance, which predicts an immediate shift of the clock forward from CT 19 to CT 22.5. Single-unit recordings demonstrated a 3.5 hr phase advance ([C2], yellow) in the SCN electrical activity rhythm after GLU treatment at CT 19 (see also Ding et al., 1994; Tischkau et al., 2000). GLU caused a 1.5 hr phase advance when applied at CT 22.5 ([C3], yellow, also see Ding et al., 1994). If KT5823 rapidly resets the clock, then application of KT5823 for 15 min at CT 22 would rapidly return the clock to CT 18.5. According to this model ([A], top), if a 30 min period is allowed for washout of KT5823, then GLU would actually be applied at CT 19, which would cause a 3.5 hr phase advance. In this case, the sum predicts that the measured phase shift would be 0 hr. Actual recordings following this experimental treatment paradigm revealed no change in phase on the subsequent day ([C5], green bar). Furthermore, if we would permit a longer interval to transpire before the second GLU pulse, the result should be different. Assuming that KT5823 applied at CT 22 rapidly returns the clock to CT 18.5, following a 3.5 hr washout period, the GLU would be applied at CT 22. This would cause an immediate 1.5 hr phase advance. The sum of these two individual shifts in clock state predicts that the measured phase shift will be a delay of −2 hr. Actual recordings show that application of GLU at CT 22 causes a 1.5 hr phase advance ([C3], yellow bar) and the sum of this double-pulse paradigm exhibited the predicted ~2 hr phase delay ([C6], green bar). Data are mean ± SEM of three to six independent experiments.

0 or after the decline in late night and were significantly reduced at predicted CT 5 compared to control samples treated with PKG-I αODN (Figure 7A). This change is consistent with the phase-resetting effects of PKG-II αODN on the electrical activity rhythm (Figure 2).

Similar results were observed in SCN slices treated continuously with PKG-II αODN and collected at CT 23, 0, and 4 as well as at CT 21 on the following day (after 44 hr in vitro) (Figure 7B). PKG-II αODN treatment significantly altered *Bmal1* levels in samples obtained at CT 23 and on the following day at CT 21. These observations are consistent with the hypothesis that the rhythm is disrupted by PKG-II αODN treatment, so that *Bmal1* cycles repeatedly through the 3.5 hr period where endogenous levels change significantly at the end of subjective night and that the *Bmal1* oscillation proceeds from this point after αODN removal.

Discussion

Our results define a critical, dynamic domain of kinase control within the circadian cycle. Whereas our initial study suggested a role for PKG at the end of the night, the data presented in this manuscript move well beyond that study to provide a specific, essential mechanism for the regulation of endogenous clock function by PKG-II. The data indicate that progression of the circadian cycle, at the levels of both core clock elements and the endogenous SCN neuronal activity rhythm, requires activation of PKG-II by intrinsic clock mechanisms. Be-

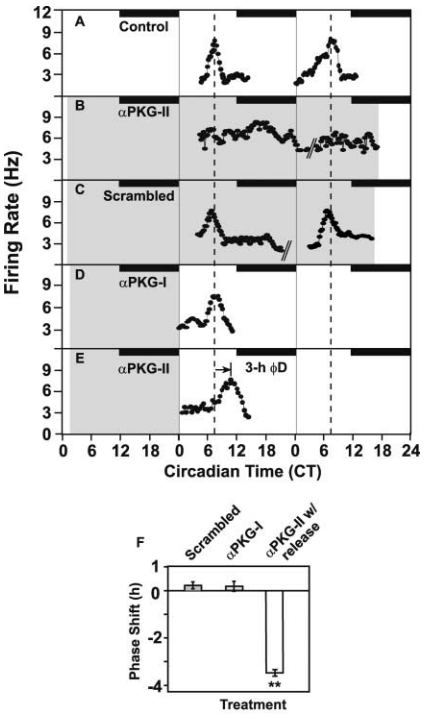

Figure 5. Continuous Inhibition of PKG-II Using αODN Disrupts the Electrical Activity Rhythm of the SCN, whereas 22 Hr Inhibition Causes Phase Delay

The horizontal black bar indicates nighttime in the donor colony; 500 μm coronal slices were maintained in constant light. Gray shading indicates the time and duration of treatment. Slices were prepared between ZT 0.5 and ZT 2. Treatment began at CT 1 in continuous αODN experiments (B and C) and at CT 2 for long-term treatments. (A) A representative single-unit recording from the ensemble of SCN neurons shows an endogenous electrical activity rhythm with a peak at ~CT 7 on both day two and day three in vitro. Mean time of peak for control experiments (n = 8) was CT 6.88 ± 0.11; this value is the phase marker to which experimentals were compared. (B) Continuous application of PKG-II αODN disrupted the SCN electrical activity rhythm on days two and three in vitro. Data were collected from a second slice on the second day of recording (indicated by the // in the record). Data are representative of five independent experiments. (C) Continuous application of a scrambled PKG-II αODN had no effect on the timing of the SCN electrical activity rhythm. Data are representative of four independent experiments. (D) Long-term application of a PKG-I αODN for 22 hr had no effect on the timing of the SCN electrical activity rhythm. Data are representative of four independent experiments. (E) Long-term application of PKG-II αODN for 22 hr caused a 3 hr phase delay in SCN activity rhythms. Data are representative of four independent experiments. Mean time of peak was CT 10.19 ± 0.16, which is significantly different from controls ($p < 0.01$, Student's t test). (F) Bar graph showing mean ± SEM for these experiments (n = 3–4). ** indicates statistical significance ($p < 0.01$) as determined by Student's t test.

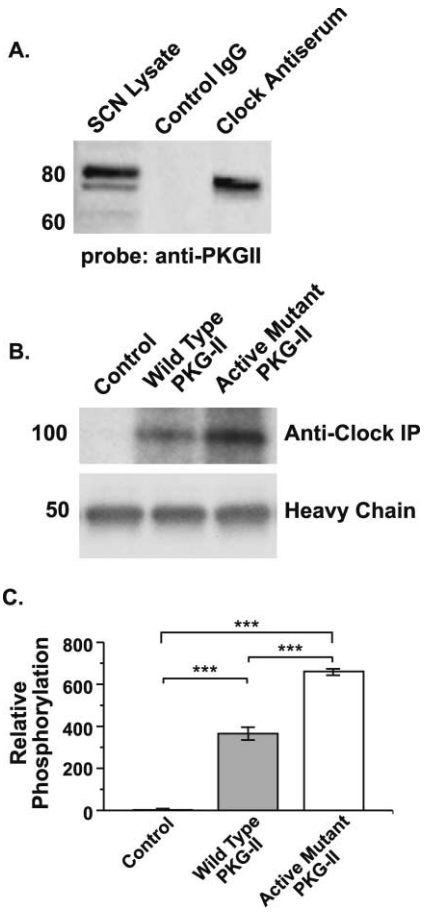

Figure 6. CLOCK Is a Potential Substrate for PKG-II

(A) SCN extracts were obtained directly from the animal at ZT 22 and subjected to immunoprecipitation by anti-CLOCK antibody. Western analysis of immunoprecipitates demonstrates an appropriately-sized band corresponding to PKG-II, suggesting an association between CLOCK and PKG-II in the SCN in vivo. Lane 1, PKG-II immunoreactivity by Western blot of SCN extract; lane 2, IgG control; lane 3, PKG-II Western blot of CLOCK coimmunoprecipitate. Data are representative of four independent experiments.

(B) Phosphorylation of CLOCK in NIH 3T3 cells cotransfected with wild-type or constitutively active PKG mutant. After incubation with 200 μCi/ml $^{32}PO_{4i}$ for 5 hr, cell extracts were immunoprecipitated with anti-CLOCK antibody and then split 1:3. Twenty-five percent was run on a gel for Western analysis of heavy chain as a control for immunoprecipitation and loading (bottom panel). Seventy-five percent was separated by SDS-PAGE and incorporated $^{32}PO_{4i}$ was determined by autoradiography. The blot is representative of three experiments.

(C) Quantitation of (B). Densitometric analysis of autoradiographs demonstrates that CLOCK shows phosphorylation when cells are cotransfected with wild-type PKG-II. CLOCK phosphorylation is increased when cells are cotransfected with a constitutively active PKG-II mutant. Data represent mean ± SEM for three experiments. *** indicates statistical significance ($p < 0.001$) between indicated pairs as determined by Student's t test.

cause clock-controlled phosphorylation events regulate core clock components (Eide et al., 2002; Garceau et al., 1997; Kloss et al., 1998, 2001; Lee et al., 2001; Lin et al., 2001; Lowrey et al., 2000; Martinek et al., 2001; Merrow et al., 1997; Myers et al., 1996; Okamura et al., 2002; Ripperger and Schibler, 2001; Zeng et al., 1994), understanding the actions of specific protein kinases within defined time domains is likely to provide fundamental insights into clock organization.

This study identifies PKG-II as an important regulator kinase, defines its regulatory influence as a narrow temporal domain at the end of the nighttime, and suggests that it acts on the positive arm of the core clockwork. Brief inhibition of the endogenous rise in PKG activity (Tischkau et al., 2003b) causes quantal delays in SCN circadian rhythms (Figure 3). Long-term knockdown of

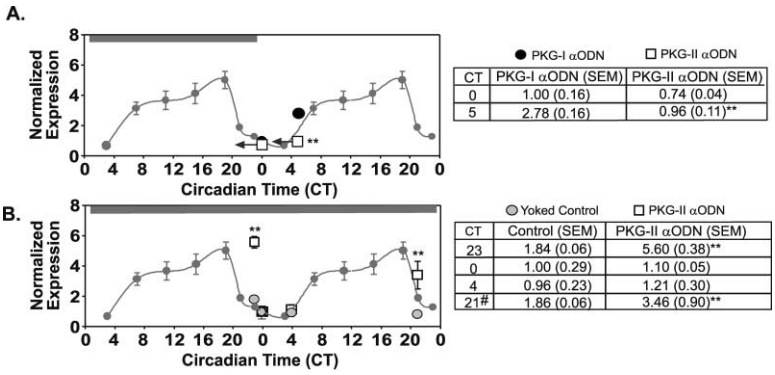

CT	PKG-I αODN (SEM)	PKG-II αODN (SEM)
0	1.00 (0.16)	0.74 (0.04)
5	2.78 (0.16)	0.96 (0.11)**

CT	Control (SEM)	PKG-II αODN (SEM)
23	1.84 (0.06)	5.60 (0.38)**
0	1.00 (0.29)	1.10 (0.05)
4	0.96 (0.23)	1.21 (0.30)
21#	1.86 (0.06)	3.46 (0.90)**

Figure 7. Inhibition of PKG-II Alters the Circadian Rhythm of *Bmal1* mRNA

The endogenous circadian profile of *Bmal1* was determined by qPCR of 500 μm reduced SCN brain slices (n = 3 for each time point, data double plotted). Shaded bars mark the time of αODN treatment. (A) Effect of 22 hr αODN treatment, followed by release. Small gray circles indicate *Bmal1* levels relative to *acidic ribosomal protein* mRNA in control SCN slices collected at the reported time points. The endogenous *Bmal1* rhythm peaked at CT 19, rapidly declined by CT 21 to a trough between CT 0–3, then increased markedly by CT 7. PKG-I or PKG-II αODN (10 μM) was applied for 22 hr, from CT 2 on day 1 in vitro to CT 24/0. SCN slices were collected 0 and 5 hr after release from αODN treatment. The *Bmal1* expression profile was not altered by PKG-I αODN (large black circles). PKG-II αODN significantly reduced *Bmal1* levels (open squares) at predicted CT 5 compared to PKG-I αODN. These levels would be expected if the clock were delayed 3.5 hr by the PKG-II αODN treatment. Arrows point to the values expected if relative expression of the *Bmal1* transcript were delayed 3.5 hr by the PKG-II αODN treatment. (B) Effect of continuous PKG-II αODN treatment throughout a 44 hr experiment until the slices were collected. This treatment is predicted to maintain the clock in a continuous 3.5 hr loop encompassing the end of night (also see Figures 3 and 8). Yoked control slices were maintained under parallel conditions, omitting αODN. *Bmal1* levels in yoked controls (large gray circles) are comparable to those measured over the first cycle in vitro. Levels under PKG-II αODN treatment (open squares) are significantly different at CT 23 and on the second day at CT 21 (after 44 hr in vitro) and match levels predicted if the clock is repeatedly delayed by 3.5 hr at the end of subjective night. Tables present the relative expression levels of the *Bmal1* transcript. # indicates that the SCN slice was in vitro for 44 hr; ** indicates statistical significance ($p < 0.05$, Student's t test) compared to time-matched controls.

PKG-II leads to arrhythmicity in electrical activity (Figure 5). Without PKG-II, the clock behaves as if locked in a dynamic loop that encompasses the biochemical state of late night. By potentially interacting with CLOCK during its phosphorylation, PKG-II may influence core clock components to signal the completion of nighttime processes and permit transit to the daytime domain. Thus, clock-controlled activation of PKG-II may serve as a critical checkpoint of temporal state at the night-to-day transition, which would align with dawn in the solar cycle.

Pharmacological studies have established a role for the cGMP/PKG signal transduction cascade activated by light/glutamate in phase resetting of the circadian clock during the second half of night (Ding et al., 1998; Liu et al., 1997; Mathur et al., 1996; Prosser et al., 1989; Weber et al., 1995). Glutamate application to SCN slices raises cGMP levels and activates PKG (S.A.T. and M.U.G., unpublished data) only when glutamate causes phase advance of the circadian clock. Inhibition of PKG activity blocks light- (Mathur et al., 1996; Weber et al., 1995) and glutamate-induced (Ding et al., 1998) phase advances in the late night but has no effect on light- or glutamate-induced phase delay in early night (Ding et al., 1998).

Clock phase is advanced if the marker of clock phase occurs earlier on the cycle(s) following a stimulus (e.g., onset of wheel running, peak electrical activity, peak expression of *Per1*) than on preceding cycles. Treatments that cause phase advance could be considered to have temporarily shortened *tau*, the period of the clock; the amount of reduction is equivalent to the phase advance. In the case of a glutamate-induced phase advance of neuronal activity rhythms, the phase advance is ~3.5 hr. Thus, *tau* on that day is 20.5 hr instead of the normal 24 hr, as that cycle has lost 3.5 hr. We hypothesized that this phase-advancing stimulus caused the clock to jump ahead to a state normally transited 3.5 hr later (Figure 8). We predict that stimuli that cause this phase advance prematurely trigger events that would be activated endogenously within the clock at this later time. In concordance with this prediction, we demonstrated clock-controlled elevation of cGMP levels and PKG activity at CT 24/0 (Tischkau et al., 2003b); increased expression of PKG-II at this time is likely a major contributor to this increase in PKG activity (Ferreyra and Golombek, 2001).

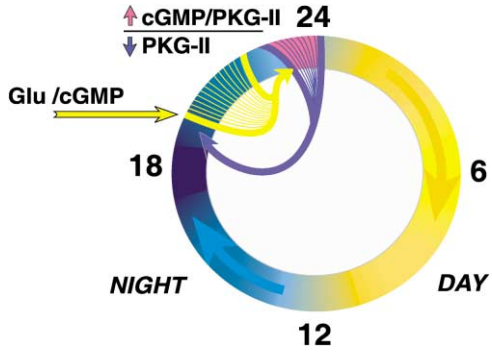

Figure 8. Model of Circadian Clock Regulation by cGMP/PKG at the End of Subjective Night

The SCN is sensitive to phase resetting by stimuli that raise cGMP and activate PKG during the last half of subjective night. When phase shifts are modeled as rapid, dynamic state changes, these stimuli would quickly set the clock forward several hours to the end of night. The rising phases of endogenous oscillations in cGMP levels and PKG activity are coincident with the waning of sensitivity to phase resetting by cGMP/PKG-dependent mechanisms. Inhibition of PKG activity during the time of the endogenous activation shifts the clock backward in the circadian cycle, into the domain of sensitivity to phase resetting by stimuli that activate cGMP/PKG (light/GLU). Thus, the endogenous rise in cGMP/PKG activity at the end of the night may act as a critical clock control point, signaling termination of nighttime processes and/or initiating the events that mediate temporal progression into the day.

Endogenous activation of PKG is critical in regulating clock timing. Inhibition of the clock-controlled increase in PKG activity causes significant phase delay of the circadian rhythm (Figure 2) (Tischkau et al., 2003b). Phase delay may be interpreted as an event that causes a transient lengthening of *tau*. There are two plausible explanations for lengthening of *tau*. First, the clock could simply be stopped for the duration of treatment. These circumstances would predict that the amplitude of phase delay would be proportional to the length of treatment. Second, the phase-delaying stimulus could actually move clock state back in time, positioning it to repeat a portion of the circadian cycle. Under these circumstances, the phase delay would equal the number of hours the clock is forced to repeat. Our data are consistent with the second hypothesis. Phase delays induced by inhibition of endogenous PKG activity are *not* proportional to the time of treatment; rather, they appear as quantal increments of 3.5 hr. Inhibition for 0.25, 1, 2, or 3 hr caused the same ~3.5 hr phase delay (Figures 3C and 3D), whereas inhibition for 3.5, 6 hr, or two pulses separated by 3.5 hr doubled this effect, delaying the electrical activity rhythm by nearly 7 hr. Because PKG inhibition with αODN reduces PKG-II protein (Figure 2H), the delay likely represents the time required to resynthesize PKG-II to a level that would reinstate the checkpoint required for the night-to-day transition. Preliminary studies indicate that PKG-II reemerges within 2 hr following cessation of treatment with the PKG-II αODN (J.W.M. and M.U.G., unpublished data). Because PKG-I αODN does not alter rhythms at this time, the end of night regulatory role is mediated by PKG-II.

If PKG inhibition at CT 22 actually resets the clock to an earlier state (CT 18.5), as predicted by our model (Figure 8), the clock should again be sensitive to the phase-advancing effect of glutamate immediately upon conclusion of treatment. When PKG inhibition at CT 22 was followed 30 min later by glutamate stimulation, the SCN neuronal activity rhythm peaked at CT 7 on the following day. These data are consistent with the summation of a phase delay induced by PKG inhibition at CT 22 followed by a phase advance induced by glutamate at CT 19. When PKG inhibition at CT 22 was followed 3.5 hr later by a glutamate stimulus, the SCN neuronal activity rhythm peaked at CT 8.5 on the subsequent day. This phase delay is consistent with summation of an ~3.5 hr phase delay induced by PKG inhibition at CT 22 and an ~2.0 hr phase advance stimulated by glutamate at CT 22. We conclude that inhibition of PKG at the end of subjective night rapidly returns the clock to a state previously transited 3.5 hr earlier (Figure 8). The return to this state permits reemergence of PKG-II activity and immediate procession of timekeeping.

Continuous exposure to αODN directed against PKG-II led to arrhythmicity of the SCN electrical activity rhythm (Figure 5). Short-term treatment with PKG inhibitors or PKG-II αODN at the end of subjective night forces repetition of the preceding 3.5 hr, during which PKG-II function is restored. Analysis of *Bmal1* mRNA levels (Figure 7) after αODN indicates that PKG-II αODN can alter a core clock element at the end of the nocturnal domain. In preliminary studies, we have seen similar effects of PKG-II αODN on *Per1* expression (data not shown), suggesting that the regulation of this checkpoint by PKG-II may affect multiple clock elements in addition to *Bmal1*. We predict that continual exposure to the PKG-II αODN deprives the clock from executing a critical temporal event and thus results in persistent repetition of the 3.5 hr preceding the transition to day. Because the clock cannot progress without PKG-II, clock state remains trapped in the nocturnal domain and rhythmicity is disrupted. Similarly, G2/M CDK inhibition or Cdc13p G2/M cyclin deletion causes repeated rounds of mitotic S phase to occur (Hayles et al., 1994; Moreno and Nurse, 1994). Thus, just as activation of G2/M CDK provides checkpoint control of the cell cycle by signaling successful completion of S phase, PKG-II may exert checkpoint control over the circadian cycle by signaling the completion of nighttime processes.

Temporal restriction of PKG-II activation and the requirement of PKG-II by the clock at the end of the night raise questions about the nature of the substrates on which it acts. In *Drosophila*, the progressive increase in apparent molecular weights of clock gene products, PER (Kloss et al., 2001; Lowrey et al., 2000; Zeng et al., 1994) and TIM (Myers et al., 1996), which occurs throughout the last half of the night, suggests that these proteins are phosphorylated prior to their degradation at the end of the night. Furthermore, FRQ, the protein product of the *Neurospora* clock gene *frequency*, undergoes similar phosphorylation events during the circadian cycle (Garceau et al., 1997). Evaluation of specific functional roles for kinases that mediate clock-controlled phosphorylation of SCN clock components (Eide et al., 2002; Martinek et al., 2001) is limited. However, the clock-controlled nature of these phosphorylation events raises the intriguing possibility that temporally restricted spheres of kinase influence, such as those described in this report, may mediate posttranslational effects on proteins critical to clock timing. We present data suggesting that PKG-II may influence rhythmicity by acting on the positive arm of the molecular clockwork. Coimmunoprecipitation studies from SCN extracts indicated that PKG-II-like immunoreactivity was present after immunoprecipitation with CLOCK. When cotransfected with PKG-II into NIH 3T3 cells, CLOCK showed increased phosphorylation that reflected relative PKG-II activity. In addition, PKG-II-driven transcription could initiate early morning accumulation of clock gene mRNAs (Panda et al., 2002), although we have not yet tested this idea. The extent to which these phosphorylation events serve as critical checkpoints paralleling the regulatory roles at transition points controlling timing and progression of cell cycle clocks (Bell and Dutta, 2002; Gitig and Koff, 2001; Yew, 2001) remains an area of active investigation.

Experimental Procedures

Animals and Circadian Time

Six- to twelve-week old LE/BluGill rats (University of Illinois) were used for these studies. Use of this inbred strain greatly reduces interexperimental variation common to outbred animals and allows the achievement of high statistical significance with small sample sizes. A dense genome scan was performed at a 10 cM interval between markers on our LE/BluGill progenitors. The results of this scan, performed by the Medical College of Wisconsin Human and

Molecular Genetics Center as part of the National Heart, Lung, and Blood Institute (NHLBI) Programs for Genomic Applications (PGA) U01 HL66579, demonstrated that the colony is inbred, yielding one allele at each locus tested (http://pga.mcw.edu/pga-bin/strain_desc.cgi).

Rats were provided food and water ad libitum and were housed under a 12:12 hr light/dark (LD) schedule; ZT 0 is defined as the time of lights on in animal colony. For SCN slices maintained under constant conditions of the brain slice chamber, circadian time (CT) is reckoned from the lighting schedule in the donor colony.

Preparation and Treatment of Brain Slices

Coronal brain slices (500 μm) were prepared at least 2 hr prior to the onset of the dark phase of the LD cycle to avoid phase shifts during preparation (Prosser et al., 1989; Prosser and Gillette, 1989). Slices containing the paired SCN were studied for up to 3 days in vitro with continuous perfusion of Earle's Essential Balanced Salt Solution (EBSS, Life Technologies, Gaithersburg, MD), supplemented with 24.6 mM glucose, 26.2 mM $NaHCO_3$, and 2.5 mg/L gentamicin and saturated with 95% O_2/5% CO_2 at 37°C (pH 7.25). Under these conditions, the SCN generates stable, near 24 hr oscillations in neuronal activity with a characteristic peak around mid-day (CT 7) (Gillette and Prosser, 1988); measurement of time of peak provides an accurate assessment of circadian phase (Gillette et al., 1995). Treatments were applied to the bath of the brain slice chamber under static bath conditions. Treatments included the specific PKG inhibitor, KT5823 (1.0 μM), or αODNs (10 μM) designed to test for PKG specificity. For continuous αODN treatment, media containing αODN was continuously perfused through the chamber, and the flow rate was reduced to ~2 ml/hr. Treatment times ranged from 0.25 to 58 hr.

Isoform-Specific PKG Antisera

Polyclonal antisera were raised in rabbit to synthetic peptides chosen to confer specificity and antigenicity for each PKG isoform. Antisera were generated against the following peptide encoding residues: PKG-1α, 51-78 of human PKG-Iα (accession number D45864); PKG-Iβ, 51-76 of human PKG-Iβ (accession number S05702); and PKG-II, 1-29 of rat PKG-II (accession number CAA85284). Peptides were synthesized at the Protein Sciences Facility (University of Illinois Biotechnology Center). Isoform specificity was confirmed by testing the immunoreactivity of each antiserum to all three PKG isoforms. PKG-Iα (bovine, recombinant *Spodoptera frugiperda*) was purchased from Calbiochem (San Diego, CA). PKG-Iβ (bovine, recombinant *baculovirus*) was purchased from Alexis Biochemicals (San Diego, CA). pCMVneo PKG-II cDNA (a gift from Dr. Michael Uhler, University of Michigan) was overexpressed in HEK cells by transient transfection using Mirus trans-it LTI transfection reagent (Madison, WI) according to the manufacturer's instructions. Additionally, specific tissues known to express or not express PKG isoforms were used to verify the isoform specificity of our antisera (data not shown). Finally, preabsorption with the synthetic peptide against which each antibody was generated resulted in the loss of the band for each respective PKG band (data not shown).

Isoform-Specific αODNs

Isoform-specific αODNs were designed to distinguish between PKG-II (5′-CCATGTTGCTCAGGA-3′) and PKG-I (5′-CCCATGCTCC TCCGG-3′). The αODN for PKG-I would affect both PKG-Iα and PKG-Iβ; however, PKG1α is not detectable in the SCN (data not shown). In addition, PKG-II-specific αODN containing one (5′-CGAT GTTGCTCAGGA-3′) or three (5′-CGATGATGCTCACGA-3′) mismatched nucleotides or scrambled sequence (5′-TCAGTACTGAG GCCT-3′) were generated for use as controls.

Western Blot

Hypothalamic brain slices (500 μM) containing the paired SCN were trimmed under a dissecting scope to preserve only the SCN and underlying optic chiasm. These "reduced" slices retain the electrophysiological and biochemical properties observed in full-size SCN slices (Gillette and Reppert, 1987). Slices were equilibrated in the brain slice chamber for at least 2 hr before the initiation of sample collection. Slices removed from the chamber at appropriate circadian times were frozen on dry ice and maintained at −80°C until analysis. Slices were homogenized in 50 μl ice-cold T-PER (Pierce) containing Complete Protease Inhibitor Cocktail (PI, Roche) and phosphatase inhibitors (Phosphatase Inhibitor Set I&II, Upstate Biotechnology) by repeat pipetting. Protein content was determined with the Micro BCA Protein Assay (Pierce). Total protein (12.5–25 μg) was resolved by 4%–15% gradient SDS-PAGE and transferred to nitrocellulose membrane. Blots were probed with PKG-Iα (1:1000), PKG-Iβ (10 μg/ml), or PKG-II (1:250) antiserum followed by goat anti-rabbit HRP-linked secondary antibodies (1:5000, Chemicon). Blots were reprobed for α-tubulin as a loading control. Blots were developed with Supersignal chemiluminescent substrate (Pierce, Rockford, IL). Digital photography and quantitation was performed with the Biochemi Analysis system (UVP).

Single-Unit Recordings of SCN Neuronal Activity

The effects of stimuli on the rhythmicity or phasing of SCN slices were assessed in vitro using the standard extracellular single-unit recording technique (Prosser et al., 1989; Prosser and Gillette, 1989). Spontaneous firing rates of individual neurons were grouped into 2 hr running averages using 15 min lags. The time of peak for each experiment was determined by visual inspection of a plot of 2 hr running averages for the symmetrically highest point. A characteristic pattern of change, such that activity was low during subjective night and peaked mid-day near circadian time 7 (CT 7, 7 hr after the onset of light in the donor colony), was observed in vehicle-treated control slices. Phase shift or, in some cases, the presence or absence of a rhythm was determined by comparing the mean time of peak from treatment groups to vehicle-treated controls. Certain recordings were performed with the experimenter blind to the treatment conditions.

Quantitative Real-Time RT-PCR

Single 500 μm SCN reduced slices were collected on dry ice immediately after treatment. Samples were placed in 1 ml TRIzol reagent (GIBCO BRL/Invitrogen, Carsbad, CA). RNA isolation was performed according to the manufacturer's protocol. Concentration and purity of the RNA was determined by UV spectrophotometry. Reverse transcription was performed in duplicate with 500 ng of total RNA in a volume of 10 μl, and 200 ng of random hexamers were added. Samples were heat denatured at 75°C for 10 min and quick chilled on ice to minimize secondary structure present in the RNA. Invitrogen Superscript II reverse transcriptase (200 U) was added along with buffer and 500 μM dNTP mix (final reaction concentration) to bring the total sample volume to 20 μl. Reactions were incubated for 1 hr at 42°C followed by a 10 min deactivation at 92°C. Samples were then diluted to 100 μl with nuclease-free water and stored at −20°C until use.

Primers were chosen using Primer Express 2.0 software (Applied Biosystems, Foster City, CA). A BLASTN search was then performed against GenBank to ensure that all primers were unique to the gene of interest. To avoid amplification from genomic DNA contamination, primer sets were designed to amplify across an intron/exon junction. *Bmal1* primers were as follows: forward, TCTATCCGATGACGAACT GAAACA; reverse, CCCTCGGTCACATCCTACGA. *Acidic robosomal protein PO* (accession number NM022402) primers were as follows: forward, CGTGATGCCCAGGGAAGA; reverse, TCCCACAATGAAG CATTTTGG.

All reactions were performed on the BioRad iCycler in triplicate with 12.5 μl SYBR Green Master Mix (Applied Biosystems, Foster City, CA), 300 nM forward and reverse primer final concentration, 5 μl of diluted RT reaction, and water to a final reaction volume of 25 μl. Initial denature was carried out at 95°C for 10 min, followed by 50 cycles of 15 s at 95°C and 15 s at 60°C. Heat disassociation was performed to check for nonspecific signals from SYBR Green and to ensure amplification specificity.

qPCR results are represented as a ratio of relative expression levels of the transcript of interest compared to a housekeeping transcript (*acidic ribosomal protein*, NM022402) used as a loading control and normalized to the value at CT 0. Relative expression levels were determined by comparing the cycle at which an arbitrary fluorescent threshold (Ct value) was reached to a standard curve for each primer set based on known RNA concentration, as described

previously (Bustin, 2000). The Ct value for a particular gene of interest was considered to be a general indicator of transcript level; threshold was placed at a value that was in the exponential portion of the amplification plot for all the products being generated and was held constant for all runs.

Coimmunoprecipitation

Single paired SCN (400 μm) were collected directly from animals sacrificed under red light at ZT 22 and frozen immediately on dry ice. Ice-cold T-PER with protease inhibitors and phosphatase inhibitors (PI/PhI, 100 μl) was added to each microfuge tube containing a SCN slice. The tube or plate was set on ice for 2 min. Slices were lysed by repeat pipetting and samples centrifuged at 10,000 RPM for 5 min at 4°C. The protein supernatant was then transferred to a new chilled microfuge tube and protein concentration derived as described above. Total protein (150 μg) was brought to a total volume of 500 μl in T-PER with PI/PhI. Protein G Sepharose (20 μl of 50% slurry, Pharmacia/Amersham, Piscataway, NJ) in T-PER with PI/PhI was added to each Co-IP sample. Antiserum (1 μg) was added to each sample. Each Co-IP was performed with the antibody of interest and an isotype control antibody to evaluate nonspecific interactions. Samples were gently rotated overnight at 4°C and were washed three times with T-PER with PI/PhI. Laemmli's Buffer (30 μl) was added and samples were heated at 100°C for 5 min and centrifuged at 14,000 RPM for 10 min. Co-IP samples along with a lysate control from the same SCN slice were resolved on a 4%–15% SDS-PAGE gel and blotted as outlined above for the antibody of interest.

In Vivo Phosphorylation

NIH 3T3 cells were transfected according to the manufacturer's instructions with JetPEI (Qbiogene, Carlsbad, CA) with the mCLOCK pCDNA expression vector (kindly provided by Dr. C. Weitz, Harvard University) and expression vectors encoding either wild-type PKG-II or a PKG-II constitutively active mutant (R118A/R119A/V125A), as indicated (PKG expression vectors kindly provided by Dr. M. Uhler, University of Michigan). The levels of DNA used in transfections were kept constant using empty control vector. Forty hours after transfection, cells were transferred for 1 hr to phosphate-free EMEM and then incubated with 200 μCi/ml $^{32}PO_{4i}$ (Perkin Elmer, Boston, MA) for 5 hr at 37°C. Cells were subjected to lysis and Co-IP with mCLOCK-specific antiserum. Washed mCLOCK immunoprecipitates were eluted in Laemmli's buffer and split 1:3. Twenty-five percent of the eluted protein was used for Western analysis of heavy chain (loading and Co-IP control), and the other 75% was separated by SDS-PAGE and analyzed after autoradiography (^{32}P incorporation).

Acknowledgments

Supported by Public Health Service Grants NS22155, NS35859, and HL67007 (M.U.G.); GM07143 (J.W.B. and J.A.B.); NS10170 (S.A.T.); NS11158 (J.W.M.); and a grant from the UIUC Governor's Venture Technology Fund/Molecular and Endocrine Pharmacology Program (S.A.T.). The authors thank P.W. Burgoon for assistance with single-unit recordings; J. Pendergast for preliminary studies; E.A. Gallman for discussion on experimental design; K. Bottum for discussion on the manuscript; K. Weis and J. Richards for technical assistance; S.C. Baker for manuscript preparation; M. Uhler for PKG-II constructs; and C. Weitz for mCLOCK expression vector. Any opinions, findings, and conclusions or recommendations expressed in this publication are those of the authors and do not necessarily reflect the views of the National Institutes of Neurological Diseases and Stroke; Heart, Lung, and Blood; or General Medicine.

Received: December 8, 2003
Revised: April 12, 2004
Accepted: July 22, 2004
Published: August 18, 2004

References

Barnes, J.W., Tischkau, S.A., Barnes, J.A., Mitchell, J.W., Burgoon, P.W., Hickok, J., and Gillette, M.U. (2003). Requirement of mammalian Timeless for circadian rhythmicity. Science *302*, 439–442.

Bell, S.P., and Dutta, A. (2002). DNA replication in eukaryotic cells. Annu. Rev. Biochem. *71*, 333–374.

Bustin, S.A. (2000). Absolute quantification of mRNA using real-time reverse transcription polymerase chain reaction assays. J. Mol. Endocrinol. *25*, 169–193.

Butt, E., Geiger, J., Jarchau, T., Lohmann, S.M., and Walter, U. (1993). The cGMP-dependent protein kinase—gene, protein, and function. Neurochem. Res. *18*, 27–42.

Comolli, J., and Hastings, J.W. (1999). Novel effects on the Gonyaulax circadian system produced by the protein kinase inhibitor staurosporine. J. Biol. Rhythms *14*, 11–19.

Ding, J.M., Chen, D., Weber, E.T., Faiman, L.E., Rea, M.A., and Gillette, M.U. (1994). Resetting the biological clock: mediation of nocturnal circadian shifts by glutamate and NO. Science *266*, 1713–1717.

Ding, J.M., Buchanan, G.F., Tischkau, S.A., Chen, D., Kuriashkina, L., Faiman, L.E., Alster, J.M., McPherson, P.S., Campbell, K.P., and Gillette, M.U. (1998). A neuronal ryanodine receptor mediates light-induced phase delays of the circadian clock. Nature *394*, 381–384.

Eide, E.J., Vielhaber, E.L., Hinz, W.A., and Virshup, D.M. (2002). The circadian regulatory proteins BMAL1 and cryptochromes are substrates of casein kinase I epsilon. J. Biol. Chem. *277*, 17248–17254.

Eskin, A., Takahashi, J.S., Zatz, M., and Block, G.D. (1984). Cyclic guanosine 3′:5′-monophosphate mimics the effects of light on a circadian pacemaker in the eye of Aplysia. J. Neurosci. *4*, 2466–2471.

Ferreyra, G., and Golombek, D.A. (2001). Rhythmicity of the cGMP-related signal transduction pathway in the mammalian circadian system. Am. J. Physiol. Regul. Integr. Comp. Physiol. *280*, R1348–R1355.

Gambaryan, S., Hausler, C., Markert, T., Pohler, D., Jarchau, T., Walter, U., Haase, W., Kurtz, A., and Lohmann, S.M. (1996). Expression of type II cGMP-dependent protein kinase in rat kidney is regulated by dehydration and correlated with renin gene expression. J. Clin. Invest. *98*, 662–670.

Garceau, N.Y., Liu, Y., Loros, J.J., and Dunlap, J.C. (1997). Alternative initiation of translation and time-specific phosphorylation yield multiple forms of the essential clock protein FREQUENCY. Cell *89*, 469–476.

Gillette, M.U. (1996). Regulation of entrainment pathways by the suprachiasmatic circadian clock: sensitivites to second messengers. Prog. Brain Res. *111*, 121–132.

Gillette, M.U., and Mitchell, J.W. (2002). Signaling in the suprachiasmatic nucleus: selectively responsive and integrative. Cell Tissue Res. *309*, 99–107.

Gillette, M.U., and Prosser, R.A. (1988). Circadian rhythm of the rat suprachiasmatic brain slice is rapidly reset by application of cAMP analogs. Brain Res. *474*, 348–352.

Gillette, M.U., and Reppert, S.M. (1987). The hypothalamic suprachiasmatic nuclei: circadian patterns of vasopressin secretion and neuronal activity *in vitro*. Brain Res. Bull. *19*, 135–139.

Gillette, M.U., Medanic, M., McArthur, A.J., Liu, C., Ding, J.M., Faiman, L.E., Weber, E.T., Tcheng, T.T., and Gallman, E.A. (1995). Intrinsic neuronal rhythms in the suprachiasmatic nucleus and their adjustment. In Circadian Clocks and Their Adjustment, D.J. Chadwick and K. Ackrill, eds. (Chichester, UK: CIBA Foundation Symposium), pp. 134–153.

Gitig, D.M., and Koff, A. (2001). Cdk pathway: cyclin-dependent kinases and cyclin-dependent kinase inhibitors. Mol. Biotechnol. *19*, 179–188.

Hayles, J., Fisher, D., Woollard, A., and Nurse, P. (1994). Temporal order of S phase and mitosis in fission yeast is determined by the state of p34cdc2-mitotic B cyclin complex. Cell *78*, 813–822.

Kloss, B., Price, J.L., Saez, L., Blau, J., Rothenfluh, A., Wesley, C.S., and Young, M.W. (1998). The *Drosophila* clock gene double-time encodes a protein closely related to human casein kinase I epsilon. Cell *94*, 97–107.

Kloss, B., Rothenfluh, A., Young, M.W., and Saez, L. (2001). Phosphorylation of PERIOD is influenced by cycling physical associations

of DOUBLE-TIME, PERIOD and TIMELESS in the *Drosophila* clock. Neuron *30*, 699–706.

Krucher, N.A., Meijer, L., and Roberts, M.H. (1997). The cyclin-dependent kinase (cdk) inhibitors, olomoucine and rocovitine, alter the expression of a molluscan circadian pacemaker. Cell. Mol. Neurobiol. *17*, 495–507.

Lee, C., Etchegaray, J.P., Cagampang, F.R.A., Loudon, A.S.I., and Reppert, S.M. (2001). Posttranslational mechanisms regulate the mammalian circadian clock. Cell *107*, 855–867.

Lin, F.-J., Song, W., Meyer-Bernstein, E., Naidoo, N., and Sehgal, A. (2001). Photic signaling by cryptochrome in the Drosophila circadian system. Mol. Cell. Biol. *21*, 7287–7294.

Liu, C., Ding, J.M., Faiman, L.E., and Gillette, M.U. (1997). Coupling of muscarinic cholinergic receptors and cGMP in nocturnal regulation of the suprachiasmatic circadian clock. J. Neurosci. *17*, 659–666.

Lowrey, P.L., Shimomura, K., Antoch, M.P., Yamazaki, S., Zemenides, P.D., Ralph, M.R., Menaker, M., and Takahashi, J.S. (2000). Positional systemic cloning and functional characterization of the mammlain circadian mutation *tau*. Science *288*, 483–492.

Martinek, S., Inonog, S., Manoukian, A.S., and Young, M.W. (2001). A role for the segment polarity gene shaggy/GSK-3 in the *Drosophila* circadian clock. Cell *105*, 769–779.

Mathur, A., Golombek, D.A., and Ralph, M.R. (1996). cGMP-dependent protein kinase inhibitors block light-induced phase advances of circadian rhythms *in vivo*. Am J. Physiol. *270*, R1031–1036.

Merrow, M.W., Garceau, N.Y., and Dunlap, J.C. (1997). Dissection of a circadian oscillation into discrete time domains. Proc. Natl. Acad. Sci. USA *94*, 3877–3882.

Michel, S., Geusz, M.E., Zaritsky, J.J., and Block, G.D. (1993). Circadian rhythm in membrane conductance expressed in isolated neurons. Science *259*, 239–241.

Moreno, S., and Nurse, P. (1994). Regulation of progression through the G1 phase of the cell cycle by the rum1+ gene. Nature *367*, 236–242.

Myers, M., Wager-Smith, M.K., Rothenfluh-Hilfiker, A., and Young, M. (1996). Light-induced degradation of TIMELESS and entrainment of the *Drosophila* circadian clock. Science *271*, 1736–1740.

Naidoo, N., Song, W., Hunter-Ensor, M., and Sehgal, A. (1999). A role for the proteosome in the light response of the timeless clock protein. Science *285*, 1737–1741.

Nurse, P. (2002). Cyclin dependent kinase and cell cycle control (Nobel lecture). Chembiochem *3*, 596–603.

Obrietan, K., Impey, S., and Storm, D.R. (1998). Light and circadian rhythmicity regulate MAP kinase activation in the suprachiasmatic nuclei. Nat. Neurosci. *1*, 693–700.

Okamura, H., Yamaguchi, S., and Yagita, K. (2002). Molecular machinery of the circadian clock in mammals. Cell Tissue Res. *309*, 47–56.

Panda, S., Antoch, M.P., Miller, B.H., Su, A.I., Schook, A.B., Straume, M., Schultz, P.G., Kay, S.A., Takahashi, J.S., and Hogenesch, J.B. (2002). Coordinated transcription of key pathways in the mouse by the circadian clock. Cell *309*, 307–320.

Pohler, D., Butt, E., Meissner, J., Muller, S., Lohse, M., Walter, U., Lohmann, S., and Jarchau, T. (1995). Expression, purification, and characterization of the cGMP-dependent protein kinases I beta and II using the baculovirus system. FEBS Lett. *374*, 419–425.

Price, J.L., Dembinska, M.E., Young, M.W., and Rosbash, M. (1995). Suppression of PERIOD protein abundance and circadian cycling by the Drosophila clock mutation timeless. EMBO J. *14*, 4044–4049.

Prosser, R.A., and Gillette, M.U. (1989). The mammalian clock in the suprachiasmatic nuclei is reset in vitro by cAMP. J. Neurosci. *9*, 1073–1081.

Prosser, R.A., McArthur, A.J., and Gillette, M.U. (1989). cGMP induces phase shifts of a mammalian circadian pacemaker at night, in antiphase to cAMP effects. Proc. Natl. Acad. Sci. USA *86*, 6812–6815.

Ripperger, J.A., and Schibler, U. (2001). Circadian regulation of gene expression in mammals. Curr. Opin. Cell Biol. *13*, 357–362.

Tischkau, S.A., Gallman, E.A., Buchanan, G.F., and Gillette, M.U. (2000). Differential cAMP gating of glutamatergic signaling regulates long-term state changes in the suprachiasmatic circadian clock. J. Neurosci. *20*, 7830–7837.

Tischkau, S.A., Mitchell, J.W., Tyan, S.H., Buchanan, G.F., and Gillette, M.U. (2003a). Ca^{2+}/cAMP response element-binding protein (CREB)-dependent activation of Per1 is required for light-induced signaling in the suprachiasmatic nucleus circadian clock. J. Biol. Chem. *278*, 718–723.

Tischkau, S.A., Weber, E.T., Abbott, S.M., Mitchell, J.W., and Gillette, M.U. (2003b). Circadian clock-controlled regulation of cGMP-protein kinase G in the nocturnal domain. J. Neurosci. *23*, 7543–7550.

Tyson, J.J., Csikasz-Nagy, A., and Novak, B. (2002). The dynamics of cell cycle regulation. Bioessays *24*, 1095–1109.

Vaandrager, A.B., Edixhoven, M., Bot, A.G., Kroos, M.A., Jarchau, T., Lohmann, S., Genieser, H.G., and de Jonge, H.R. (1997). Endogenous type II cGMP-dependent protein kinase exists as a dimer in membranes and can be functionally distinguished from the type I isoforms. J. Biol. Chem. *272*, 11816–11823.

Weber, E.T., Gannon, R.L., and Rea, M.A. (1995). cGMP-dependent protein kinase inhibitor blocks light-induced phase advances of circadian rhythms *in vivo*. Neurosci. Lett. *197*, 227–230.

Welsh, D.K., Logothetis, D.E., Meister, M., and Reppert, S.M. (1995). Individual neurons dissociated from rat suprachiasmatic nucleus express independently phased circadian firing rhythms. Neuron *14*, 697–706.

Yang, Y., Cheng, P., Zhi, G., and Liu, Y. (2001). Identification of a calcium/calmodulin-dependent protein kinase that phosphorylates the Neurospora circadian clock protein FREQUENCY. J. Biol. Chem. *276*, 41064–41072.

Yew, P.R. (2001). Ubiquitin-mediated proteolysis of vertebrate G1- and S-phase regulators. J. Cell. Physiol. *187*, 1–10.

Zeng, H., Hardin, P.E., and Rosbash, M. (1994). Constitutive overexpression of the *Drosophila period* protein inhibits *period* mRNA cycling. EMBO J. *13*, 3590–3598.